ELSEVIER

Image and Vision Computing 18 (2000) 397–413

image AND vision COMPUTING

www.elsevier.com/locate/imavis

CLARK: a heterogeneous sensor fusion method for finding lanes and obstacles

M. Beauvais, S. Lakshmanan*

Department of Electrical and Computer Engineering, University of Michigan—Dearborn, Dearborn, MI 48128-1491, USA

Received 31 March 1999; received in revised form 28 August 1999; accepted 14 September 1999

Abstract

This paper describes Combined Likelihood Adding Radar Knowledge (CLARK), a new method for detecting lanes and obstacles by fusing information from two forward-looking vehicle mounted sensors—vision and radar. CLARK has three stages: (1) obstacle detection using a novel template matching approach; (2) lane detection using a modified version of the Likelihood Of Image Shape algorithm; (3) simultaneous estimation of both obstacle and lane positions by locally maximizing a combined likelihood function.

Experimental results illustrating the efficacy of these components are presented. CLARK detects the position of lanes and obstacles accurately, even under significantly noisy conditions.

Keywords: Bayesian detection; intelligent vehicles; deformable templates; global shape matching

1. Introduction

1.1. Background and problem statement

There is a desire among consumers worldwide for automotive accessories that make their driving experience safer and more convenient. It is widely accepted that automotive safety accessories will have a tremendous payoff to society at large—see [1–4] for details. In response to this, the automotive industry in cooperation with government agencies has embarked on programs to develop new safety and convenience technologies [5]. These include, but are not limited to, collision warning (CW) systems, lane departure warning (LDW) systems, and intelligent cruise control (ICC) systems. These systems and others comprise an area of study referred to as intelligent transportation systems (ITS), or more broadly, intelligent vehicle highway systems (IVHS) [5].

This paper is concerned with improving the state-of-art of ITSs such as ICC, CW, and LDW systems, especially in terms of improving their reliability/robustness. Before stating the main goals of this paper, a discussion of the failure modes for current systems is in order. Take ICC and CW systems for instance—many current prototypes being tested are not reliable under some common driving scenarios, namely curved roadways (see Fig. 1). The prototypes all use a staring monobeam range/proximity sensor with a very narrow beam width to determine the distance to the vehicle ahead. On a curved portion of roadway, the vehicle ahead could easily move outside of the sensor's footprint. This could cause an ICC system to accelerate inappropriately. If the lead vehicle decelerated or if another vehicle entered the driver's path on the curved road, a CW system might not respond until the driver had gone inside of the safe stopping distance, creating the potential for a collision. Also, along curved stretches of highway, the radar system may detect traffic in adjacent lanes or even roadside clutter such as guard-rails, etc. as the vehicle/obstacle ahead. This could cause an ICC/CW system to produce false alarms that further decrease their reliability. ICC and CW systems are also unreliable in cases where the road is not reasonably flat. In cases where the road in front of the radar sensor is sloped upward, due to either a hill or a banked turn, the proximity sensor can falsely detect the road as an obstacle. Several filtering/tracking methods for correcting such failures have been proposed [6] and seem to work well for certain situations, but not adequately enough to ignore the problem.

Failure modes are by no means applicable to ICC and CW systems alone; LDW systems also have problems with common driving scenarios. LDW systems that rely on a side looking camera (i.e. they only detect the position of the lane next to the vehicle) have trouble accounting for curves in the roadway and for variations in the individual driving patterns [7]. LDW systems that use a forward-looking

* Corresponding author. Tel.: +1-3135935516; fax: +1-3135939967.

E-mail addresses: michelab@umich.edu (M. Beauvais), lakshman@umich.edu (S. Lakshmanan).

0262-8856/00/$ - see front matter
PII: S0262-8856(99)00035-9

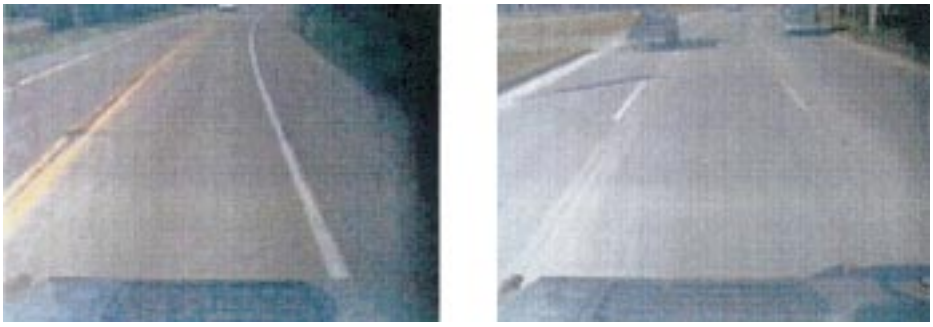

Fig. 1. Examples of driving scenarios that cause false alarms in ICC and CW systems.

camera (i.e. they estimate the entire geometry of the lane in front of the vehicle) have accuracy problems at far distances [8]. All of this results in incorrect estimates for the time-to-lane-crossing (TLC) estimate. Attempts have been made to remedy the failures using additional dead reckoning and driver behavior information, but here too the problem has not been adequately resolved.

This leads up to the two central questions of this paper:

Is there a robust method for detecting obstacles in front of a vehicle so that both the obstacle's range as well as its lane status/relevance is known? How can information about obstacles be used to increase the accuracy of the estimate of lane's geometry?

Currently, ICC and CW systems detect the presence and the range of obstacles ahead by using the range/proximity sensor alone [9–12]. Hence, the lane status/relevance of that obstacle is unknown. Similarly, current LDW systems estimate lane geometry using the data from the camera alone [13–17], without any prior knowledge regarding obstacles.

1.2. CLARK

This paper presents a new method called Combined Likelihood Adding Radar Knowledge (CLARK) for accurate estimation of both obstacle positions and lane locations using information from the range/proximity sensor as well as the video camera simultaneously. CLARK comprises of two principal components:

1. The robust detection of obstacles through multi-sensor and multi-feature fusion;
2. Incorporating this information into the Likelihood Of Image Shape (LOIS) lane detection algorithm to improve LOIS' estimate of the lane's position at far ranges as well as further refine the position of the detected obstacle.

First, the obstacle detection component: obstacles are essentially found in the visual image, however, the search is constrained by range information from the radar (proximity) sensor. A rectangular obstacle template is constructed and the decision as how to deform it (where precisely to place the template in the image) is influenced by the information contained in the image's intensity gradient field and its color field. Three parameters of the rectangular box are allowed to vary—left edge, bottom edge and width.[1] The objective is to deform the obstacle template using these three parameters so that it is placed over portions of the image where the intensity gradient is large in magnitude and also perpendicular to the template edges, and where the difference in color (measured by the Fisher distance) between portions of the image that are inside and outside of the template is maximum. Deformations of the template that keep its position close to the radar measurement are preferred over those that move the template further away from the measurement. An experimental result of obstacle detection using the method above is shown in Fig. 2 in order to illustrate the procedure.

After the obstacle has been detected, the second component of CLARK becomes effective. Information regarding the already detected obstacle is integrated into a lane finding algorithm. The lane finding algorithm used throughout this paper is LOIS. LOIS finds lanes in images by using a deformable lane edges should be in portions of the image where the intensity gradient is large in magnitude and whose orientation is perpendicular to the lane edge—see [8] for details. The integration of obstacle information into the standard LOIS is first attempted by a simple process of data masking. Pixels that are part of the detected obstacles are masked out, so that their image gradient values do not influence LOIS' likelihood at all. This strategy has some advantages, as it prevents LOIS from 'locking-on' to edges that are not part of the lane but of an obstacle in front of the vehicle (see Fig. 3). However, when the true lane edges are very close to the obstacle edges (as is the case when the vehicle is directly ahead and the road is perfectly straight, for example), the masking technique backfires (see Fig. 4).

For the masking technique to be effective, a compromise has to be reached between the obstacle and the lane detection stages. This compromise involves a combined likelihood. Rather than fix the position and size of the detected obstacle, these parameters are instead allowed to vary within a narrow range around their individually determined values. The new likelihood is a combination (product) of the

[1] The height of the rectangular template is always assumed to be the same as its width.

Fig. 2. Left: a color image with a vehicle in the FOV, and the radar measurement overlaid (green dot). Middle: result of obstacle detection performed using the image intensity gradient field alone (shown as red box). Right: the improvement in obstacle detection by adding color information.

standard LOIS likelihood and the obstacle detection likelihood, and it is maximized using a seven-dimensional (three-dimension for the obstacle and four-dimension for the lane) search. This new search determines the best estimate of the obstacle and the lanes simultaneously and constitutes the method called CLARK in this paper (see Figs. 5–7 for some sample results that illustrate the efficacy of CLARK).

In addition to the assumptions made because of using the LOIS algorithm (see Section 2), several additional ones are made and used in this paper. These additional assumptions are listed below:

- Obstacles are assumed to be rectangular in shape and have a minimum size (approximately one-half of a standard lane wide). Passenger cars, vans, trucks, and buses all obey this assumption. However, motorcycles, bicycles, and pedestrians do not, and would probably not be detected by CLARK.
- The rectangular shape assumption is also influenced by the radar system used in this paper. This system has a fixed single narrow radar beam looking directly in front of the vehicle, and so it is assumed that any obstacle detected by this system has a rectangular pose/appearance in the image plane. If the system had a wider beam as in [18], or has a scanning radar as in [9], or has multiple beams as in [19], then the rectangular pose/appearance assumption would not be valid.
- The radar system used influences another assumption as well, namely the one of deciding precisely where the obstacle detected by it is. In this paper, we assume that the lateral position of the detected obstacle is always at the center of the radar beam.

1.3. Literature survey of obstacle detection research

There has been a large body of research in the field of object detection. The objects of interest in applications relating to ITS are obstacles (vehicles, pedestrians, etc.), and this survey is undertaken with that in mind. The first consideration for obstacle detection involves the choice of sensor modality. There does not seem to be a consensus on

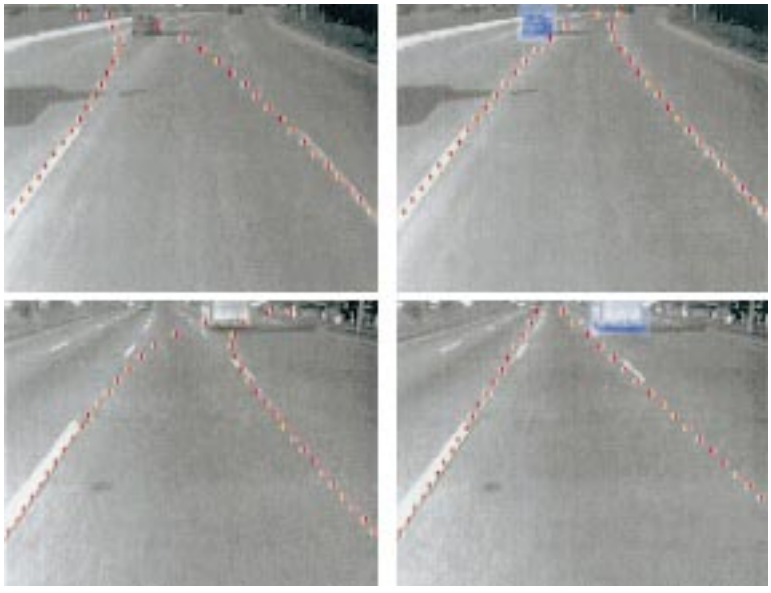

Fig. 3. Left: Lane detection results using the standard LOIS. Right: LOIS' results on the same images when the detected obstacles are masked during lane detection.

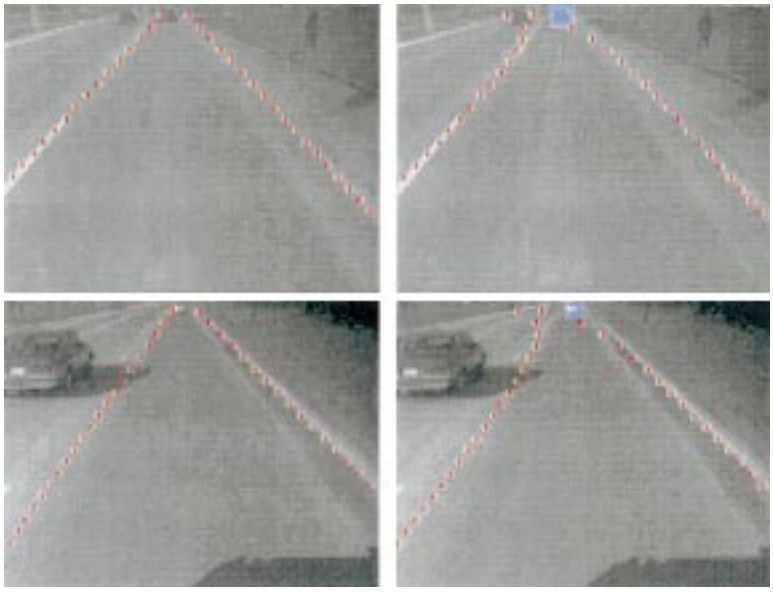

Fig. 4. Left: Lane detection results using the standard LOIS. Right: LOIS' results on the same images when the detected obstacles are masked during lane detection.

Table 1
Summary of various sensor characteristics

Sensor type	Advantages	Disadvantages
Ultrasound	Inexpensive	Poor range capability
	Insensitive to darkness	Sensitive to weather conditions
Vision	Multiple target recognition and classification	No direct range determination
	Good resolution	Complex algorithms—slow processing
	Compact equipment	
Laser radar	Relatively inexpensive	Technical problems remain
	Insensitive to darkness	Sensitive to water/dirt/ambient light
MMW Radar	Insensitive to light and weather	Expensive

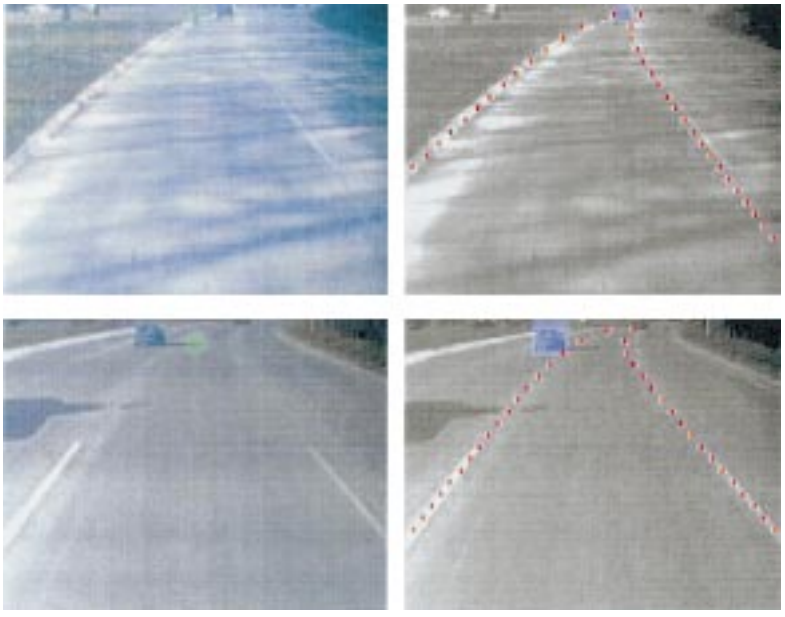

Fig. 5. Classifying obstacles according to their lane relevance using CLARK. CLARK determines the obstacle to be—top: in the same lane, and bottom: not in the same lane.

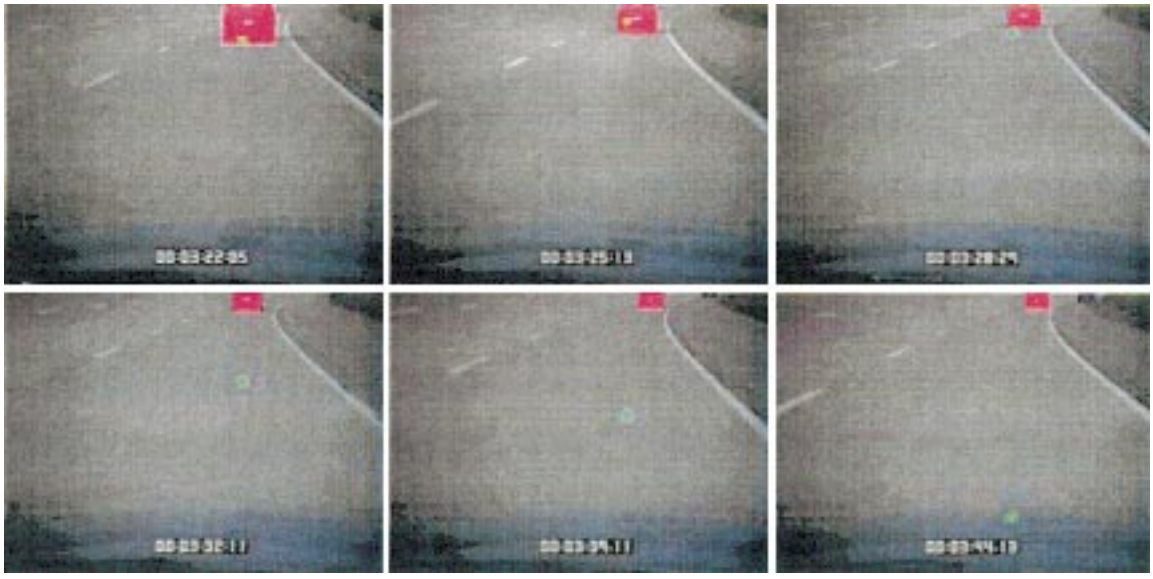

Fig. 6. Obstacle detection and tracking using CLARK.[2]

which modality offers clear advantages for ITS, as each of them have some advantages as well as disadvantages (see Table 1).

The simplest modality used for obstacle detection is the ultrasound, or sonar, sensor. Ultrasound sensors work by bouncing a sound pulse off an object and determining the range of the object from the round trip time. They are widely used in mobile robotics applications [20]. The strength of ultrasound as a sensor modality for obstacle detection lies in the fact that they are cheap, easy to use, and give accurate range estimates for up to 10 m. For ITS applications, however, ultrasound is not a very suitable modality except for some limited scenarios described in [21]. First, ultrasound sensors operate reliably only until 10 m, so that limits their use for highway applications. Second, they operate at the speed of sound, so even if their range capability can somehow be extended, to 100 m for example, their update rate for obstacles in the 100 m range would be no faster than 2 Hz. This latency limits their use for highway applications. These problems, coupled with the fact that sound pulses attenuate rapidly in air and are easily interfered with by wind and other sound sources, make the ultrasound sensor impractical for any forward-looking CW/ICC applications on highways.

Visual modality sensors, on the other hand, are quite popular for use in CW systems.[3] The advantages of using visual modality sensors are that they are small in size, reasonably cheap, and can detect multiple objects over a wide range and field-of-view. The information contained in the images obtained from such sensors also allows the classification of detected obstacles according to their size and shape. Several different algorithms have been developed for obstacle detection in visual modality sensors. Some of these are template-based. They exploit the differences in intensities between pixels (i.e. the intensity gradient field) to fit the template to image edges [22–25]. However, these methods have difficulties in reliably locating obstacles when there are other 'noise' edges (such as from shadows, roadside clutter, etc.) that mimic those of an obstacle. More complex algorithms incorporate color to aid in the detection of obstacles. Ref. [26] uses a color-based blob analysis method along with optical flow techniques to detect and track vehicles. Ref. [27] uses a non-parametric color classification method to segment obstacles from the background via a multivariate decision tree. The inclusion of color increases the reliability of the obstacle detection, but only at the cost of additional computation, as color images have three times as much information as gray tone images. A more recent approach to obstacle detection is stereo vision (see [28,29]) where images obtained from two cameras placed within a known parallax of each other are used to triangulate obstacles. A major advantage of stereo vision techniques is that they provide obstacles' range, as opposed to the usual single camera techniques; but on the other hand, they are computationally demanding.

Radar based range sensing has been the modality of choice in military and aerospace applications for several decades. The principal advantage of using radars is that they can robustly detect the range of obstacles, independent of weather or lighting conditions. In the last decade or so the size and cost of radar sensors have been reduced to such a level that commercial automotive applications are now

[2] A running time estimate of the standard deviation in the radar-based range measurement (overlaid in a green dot), is used to determine the extent to which the rectangular obstacle template is allowed to deform in the visual image.

[3] Afer all, humans use their vision as the primary mechanism for detecting obstacles while driving, so it is reasonable to assume that a system mimicking such a human activity could also do it by using the same modality.

thought feasible [30]. Depending on the application and the associated cost, several varieties of radar systems have been developed—those that detect single targets or multiple targets, those that operate at low frequency or higher frequency, etc. [31]. Perhaps the simplest and cheapest radar sensor is the ultra-wideband ground-penetrating impulse radar, or "radar on a chip", developed recently at Lawrence Livermore National Labs [18]. This system acts like a proximity sensor, detecting when an object moves inside a preset range to the sensor. With the correct hardware, this device can be made to scan a range of distances up to a maximum of about 15 m, and produce very accurate range measurements. The radar pulse output times are randomized, preventing multiple sensor interference. While this sensor is inexpensive (less than US$100), its usefulness for highway-based ITS applications is limited by its short range (much like an ultrasound sensor). Fixed narrow ($\sim$2–10° vertical and azimuth) monobeam radar systems with a maximum range of well over 100 m (like the ones in Refs. [10,12]) are perhaps the most popular in this sensing modality. Systems of this type are still relatively inexpensive and robust, but lack azimuth (angle) information about obstacles and so suffer from false alarm and error problems. Another ongoing concern with this type of radar is that multiple systems in the same area may interfere with one another. Overcoming these problems requires the ability to distinguish multiple targets in both range and azimuth. This is accomplished by using either a scanning or a multiple-beam radar system [9,11,17], although only with an associated increase in the system's cost.

Laser-based radars as the sensor modality for obstacle detection are very appealing due to the availability of cheap sensors. As a simple ranging system, they are nearly as robust as radar systems, but lower in cost. Laser radar systems work by bouncing a pulse of light off of an object and measuring the phase shift of the reflected signal to determine distance. When combined with a mechanical horizontal scanning unit, these systems can be used to determine the range of objects over a wide set of azimuth angles fairly inexpensively [32,33]. However, laser radar based ranging systems do have some serious drawbacks. Although they can operate under poor lighting conditions, their optics are sensitive to dirt and water. Also, the reflection coefficients of obstacles vary so much that these systems can become easily confused between highly reflective road elements (such as newly painted road) and poorly reflecting obstacles of interest.

In order to overcome the disadvantages of using individual sensors, there has been some work done on combining information from different sensor types. The field of autonomous robot navigation contains several references [34–36] that combine range information from an ultrasound sensor with azimuth information from an image sensor in order to detect obstacles more reliably than by using just one of those sensors. More recently, Ref. [37] combines information about the range and azimuth position of potential obstacles from a high-resolution radar sensor with the azimuth position of potential obstacles determined independently by a vision sensor (using a color blob flow analysis algorithm). Ref. [32] develops a collision warning system that combines a scanning laser radar with a single color camera. The vision algorithm uses edge-based histograms to detect obstacles and lanes, and computes the distance to these objects using the laser radar.

1.4. Literature survey of lane detection research

Lane detection, the problem of locating lanes in front of a vehicle with no prior estimate to focus the search, is an important enabling or enhancing technology in a number of intelligent vehicle applications, including lane departure warning, intelligent cruise control, lateral control, and ultimately autonomous driving. Work in this area has primarily been focused on vision based techniques, as the strongest lane cues are colored lane stripes that can most robustly be detected visually. Some related work has been done on detecting road boundaries with radar, such as those in [38,39].

Many systems for vision based lane detection are described in the literature. The first generation of these lane detection systems was edge-based. They relied on thresholding the image intensity to detect potential lane edges, followed by a perceptual grouping of the edge points to detect the lane markers of interest. A number of these systems make the assumption that the lane boundaries are straight lines, and detect them by extracting edge points from the image and using the Hough transform. An example of such a system is a lane detector developed in [40]. The system developed in [11] and later versions of the LANELOK system developed in [13] enforce a global scene constraint between the left and right lane edges (that they should meet at a vanishing point on the horizon row in the image plane). The system in [15] further extends these methods to better handle curved roads by dividing the image into a small number of horizontal sections and finding linear approximations to the lane edges within each section.

The first generation systems suffered from many problems. The use of a linear or piecewise-linear model of the lane boundaries severely limited their accuracy. There was another, and perhaps more important, deficiency with them regarding image thresholding. In many road scenes, it is not possible to select an intensity threshold, which eliminates the detection of noise edges without also eliminating the detection of true lane edge points. Therefore, these first generation lane detection systems that relied excessively on edges detected by thresholding the intensity gradient field suffered when the images contained extraneous edges due to imperfections in the road surface such as vehicles, on/off ramps, puddles, cracks, shadows, oil stains, etc. The same structural problem also applied when the lanes were of low contrast, broken, occluded, or totally absent.

The second generation of systems sought to overcome

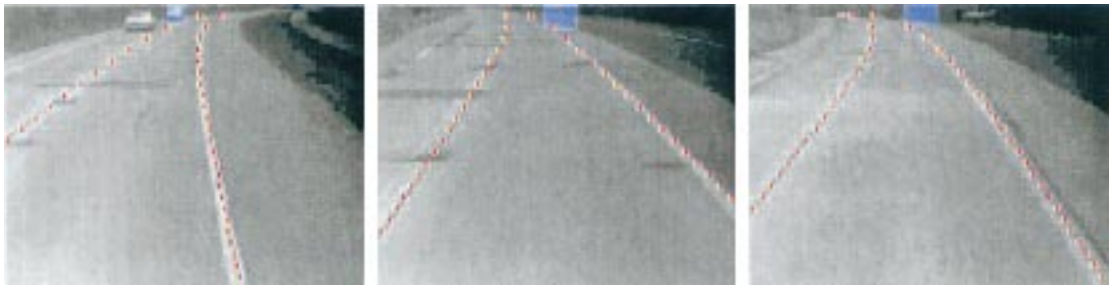

Fig. 7. Additional examples of lane and obstacle detection using CLARK.

this distraction problem by using a global model of lane shape in conjunction with the raw image intensity array, as opposed to separately detecting and grouping edge points. One example of a second generation system is ARCADE [14]. ARCADE uses global road shape constraints derived from an explicit model of how the features defining a road appear in the image plane. A simple one-dimensional edge detection is followed by a least median squares technique for determining the curvature and orientation of the road. Individual lane markers are then directly determined by a segmentation of the row averaged image intensity values. ARCADE, unlike its predecessors, does not require any perceptual grouping of the extracted edge points into individual lane edges. The RALPH system [16] is another example of a second generation lane detection system. Like ARCADE, RALPH also uses global road shape constraints. The crux of RALPH is a matching technique that adaptively adjusts and aligns a template to the averaged scanline intensity profile, in order to determine the lane's curvature and lateral offsets. The LOIS lane detector [8], yet another example of a second generation lane detection system, uses template matching as well. However, unlike RALPH, LOIS' match is over the entire image and not just an averaged scan line. LOIS uses a likelihood function that encodes the knowledge that the edges of the lane should be near intensity gradients whose orientations are perpendicular to the lane edge. LOIS will be discussed in further depth in Section 2. There are several other such second generation systems—see [41].

As a group, these second generation systems have been subject to testing that involved the processing of extremely large and varied data sets. These tests have shown that the second generation lane detection systems perform significantly better in comparison to those of the first generation. However, the problems associated with the first generation systems have not been entirely overcome. In particular, a number of second generation lane detection systems still have a tendency to be 'distracted' or 'pulled' away from the true lane markers by the presence of strong and structured edges, such as those created by a vehicle outline. In portions of the image whose distance from the camera is large, vehicle outlines have a higher contrast compared to the true lane markers (see middle column of Fig. 8) due to the foreshortening effect. In such cases, lane hypotheses that include the vehicle outline are more favored than those that do not include them. This 'distraction problem' is illustrated

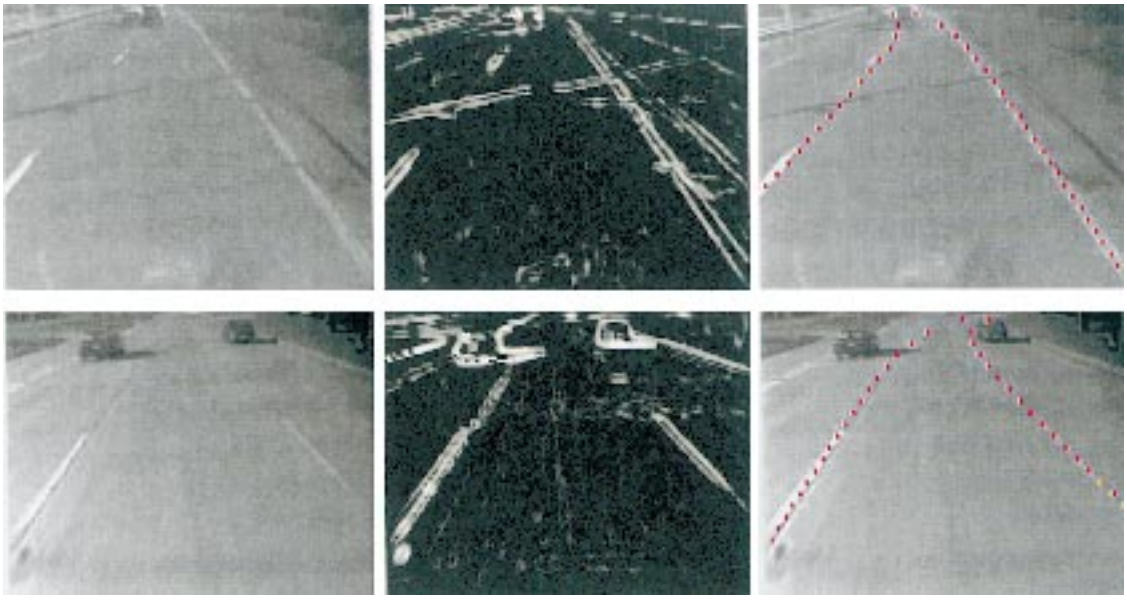

Fig. 8. Examples of LOIS becoming distracted by non-lane objects that have large gradient magnitudes.

in Fig. 8, which shows two example images where the LOIS lane detection algorithm determines that a hypothesis that includes the vehicle outline as part of the template as being the best among all possible hypotheses. This 'distraction problem' is further complicated by the fact that vehicles in the current lane reinforce the correct lane hypothesis, provided the lanes are reasonably straight.

Therefore, although second generation lane detection systems provide a fairly accurate estimate of the vehicle's offset and orientation relative to the true lane markers, their curvature estimates are not reliable. One possible way to overcome this problem is to find image features that include the same amount of information about the true lane markers as the image intensity gradient field, but are not as sensitive to extraneous edges. LANA [42] does this by using frequency domain features to differentiate true lane markings from other structured edges. Another way is to provide information about obstacles ahead of the vehicle to the lane sensing system in order to avoid corrupting the gradient field data that is used to estimate the lane shape parameters. Several algorithms have been developed to fuse lane and obstacle information to reduce ICC/CW false alarms (see [16,22,28,32,33]). Although such algorithms use lane information to determine the lane relevance of the vehicles/obstacles ahead, none of them do the reverse, namely, use the information about vehicles/obstacles ahead to help detect lanes better.

1.5. Main contributions of this paper

A consolidation of the main contributions of this paper is now in order. As described in Section 1.1, this paper is concerned with the problem of detecting obstacles and lanes in common roadway scenarios, as a precursor to an ICC/CW system. This paper adds two contributions:

- The first is the novel manner in which multiple modalities are fused to detect obstacles. The use of range information combined with edge data with a deformable template allows the robust tracking of obstacles. The addition of Fisher color distance information eliminated the problem of strong gradients caused by shadows, lanes, cracks, etc. Limiting the use of this information to areas around 'likely' hypotheses allows on-the-fly calculations; no training sets or precomputed color transforms are necessary.
- The second is the joint likelihood model, in which a combined obstacle and lane likelihood function is optimized. This joint likelihood model increases CLARK's efficacy by allowing the obstacle position estimate to influence the lane position estimate, and vice versa. Past algorithms detected these two features independently.

The rest of this paper is organized as follows. Section 2 presents an overview of LOIS, followed by Section 3 that provides details on CLARK—the method used to detect obstacles and then integrate that obstacle information into LOIS. Numerous experimental results are presented along with every section of this paper. Concluding remarks and some possibilities of future research are presented in Section 4.

2. Lane detection using LOIS

LOIS uses a deformable template approach to lane detection. The deformable template approach to object detection has three components: a parametric family of shapes which describes the possible ways that lane markers can appear in the image, a likelihood function which measures how well a particular hypothesized lane shape matches a given image, and a method for finding the shape parameters which maximizes that likelihood function. Each of these components is described in detail below.

2.1. Defining a class of parametric lane shapes

Assume that the lane edges are circular arcs on a flat ground plane. For small to moderate curvatures, a circular arc with curvature k can be closely approximated by a parabola of the form

$$x = \frac{1}{2}ky^2 + my + b \tag{1}$$

The derivation of the class of corresponding curves in the image plane is given for the case of an untilted camera, but it can be shown that the same family of curves results when the camera is tilted. Assuming perspective projection, a pixel (r,c) in the image plane projects onto the point (x,y) on the ground plane according to the two equations

$$x = cc_f y \tag{2}$$

$$y = \frac{H}{rr_f} \tag{3}$$

where H is the camera height, r_f is the height of a pixel on the focal plane divided by the focal length, and c_f is the width of a pixel on the focal plane divided by the focal length. Substituting Eqs. (2) and (3) into Eq. (1) and performing some simple algebraic manipulation results in the image plane curve

$$c = \frac{kH}{2r_f c_f r} + \frac{br_f r}{Hc_f} + \frac{m}{c_f} \tag{4}$$

or, combining the ground plane and camera calibration parameters together,

$$c = \frac{k'}{r} + b'r + vp \tag{5}$$

In the case of a tilted camera, the same family of curves results if the image coordinate system is defined so that row 0 is the horizon row. For left and right lane edges defined by concentric arcs, the approximation is made that the arcs have equal curvature and equal tangential orientation

where they intersect the X axis, so k' and vp will be equal for the left and right lane edges. While the radius of curvature and tangent orientation of the left and right lane edges will differ slightly, constraining the left and right lane edges to have the same k' and vp parameters closely approximates the actual lane edge shapes for all but very small radii of curvature. As a result, the lane shape in an image can be defined by the four parameters k', b'_{LEFT}, b'_{RIGHT} and vp. The k' parameter is linearly proportional to the curvature of the arc on the ground plane. The vp parameter is a function of the tangential orientation of the arc on the ground plane, with some coupling to the arc curvature as well (depending on the amount of camera tilt). The b'_{LEFT} and b'_{RIGHT} parameters are functions of the offset of the arc from the camera on the ground plane, with couplings to arc curvature and tangential orientation (again, the relative contributions of these couplings depend on the camera tilt).

2.2. The likelihood function

The intuition underlying the likelihood function used by LOIS is that there should be a brightness gradient near every point along the lane edges. The larger the magnitude of that gradient, the more likely it is to correspond to a lane edge. Also, the closer the orientation of that gradient is to perpendicular to the lane edge, the more likely it is to correspond to a lane edge. This likelihood function operates on raw image gradient information without the need for explicit thresholding to select edge points. As a result, weak edges with consistent gradient orientations can support the correct lane shape hypothesis, while strong edges with inconsistent orientations (such as those resulting from shadows) do not distract LOIS from finding the correct lane shape.

More formally, define the penalty function (or spike-weight function)

$$f(\alpha, x) = \frac{1}{1 + \alpha * x^2} \tag{6}$$

where α determines how fast $f(\alpha, x)$ decreases as x increases. Then the contribution of each pixel to the likelihood value is equal to

$$\text{GradMag}_{\text{pixel}} * f(\alpha_1, \text{Dist}_{\text{pixel}}) * f(\alpha_2, \cos[\text{GradOrtn}_{\text{pixel}} - \text{TempTgt}]) \tag{7}$$

where $\text{Dist}_{\text{pixel}}$ is the distance in columns from the closest lane edge (left or right), and TempTgt is the tangential orientation of the closest template lane edge calculated for the pixel's row. The calculation of the likelihood function clips the portions of the image more than a specified distance from the hypothesized lane edges in order to increase the speed of the function. Also, look-up tables are used for $\cos(\cdot)$ and the penalty function $f(\cdot)$ in order to further increase the speed of the likelihood function calculation.

2.3. Map estimation and the metropolis algorithm

Real world lanes are never too narrow or wide. Accordingly, a prior probability density function (pdf) is constructed over the space of lane shape parameters k', b'_{LEFT} b'_{RIGHT}, and vp:

$$P(k', b'_{\text{LEFT}}, b'_{\text{RIGHT}}, vp) \propto (a \tan[b'_{\text{RIGHT}} - b'_{\text{LEFT}} - 1] - a \tan[b'_{\text{RIGHT}} - b'_{\text{LEFT}} - 3]) \tag{8}$$

to reflect that a priori knowledge.

It is also assumed that given the values of k', b'_{LEFT} b'_{RIGHT}, and vp, the probability of the given image having a certain intensity gradient field is given by the likelihood pdf:[4]

$$P(\text{Observed Image}|k', b'_{\text{LEFT}}, b'_{\text{RIGHT}}, vp) \propto \sum_{i,j} \text{GradMag}_{i,j} * f(\alpha_1, \text{Dist}_{i,j}) * f(\alpha_2, \cos[\text{GradOrtn}_{i,j} - \text{TempTgt}]), \tag{9}$$

This likelihood pdf encodes the knowledge that the true lane markers lie along portions of the image that uniformly have a high intensity gradient field whose orientation is perpendicular to the lane edges.

These two pdfs are combined using Bayes' rule, and the lane detection problem is reduced to one of finding the global maximum of a posterior pdf (i.e. the MAP estimate):

$$\begin{aligned}
&\underset{k', b'_{\text{LEFT}}, b'_{\text{RIGHT}}, vp}{\text{argmax}} \; P(k', b'_{\text{LEFT}}, b'_{\text{RIGHT}}, vp|\text{Observed Image}) \\
&= \underset{k', b'_{\text{LEFT}}, b'_{\text{RIGHT}}, vp}{\text{argmax}} \; P(k', b'_{\text{LEFT}}, b'_{\text{RIGHT}}, vp) \\
&\quad \times P(\text{Observed Image}|k', b'_{\text{LEFT}}, b'_{\text{RIGHT}}, vp) \\
&= \underset{k', b'_{\text{LEFT}}, b'_{\text{RIGHT}}, vp}{\text{argmax}} \; (a \tan[b'_{\text{RIGHT}} - b'_{\text{LEFT}} - 1] \\
&\quad - a \tan[b'_{\text{RIGHT}} - b'_{\text{LEFT}} - 3]) \times \sum_{i,j} \text{GradMag}_{i,j} \\
&\quad * f(\alpha_1, \text{Dist}_{i,j}) * f(\alpha_2, \cos[\text{GradOrtn}_{i,j} - \text{TempTgt}])
\end{aligned} \tag{10}$$

In general, the RHS of Eq. (10) is not a concave function, and often contains several local maxima. As a result, local optimization techniques such as gradient descent are not appropriate. The standard implementation of LOIS uses the Metropolis algorithm with a geometric annealing schedule [43] to perform this maximization (see [8,44,45]

[4] Ideally, the likelihood pdf should also contain a normalizing factor that depends on the lane shape parameters. However, calculating this factor is very difficult, as it involves an integration of the RHS of Eq. (9) over all values of the gradient field. Omission of such a factor is ubiquitous to Bayesian methods in image analysis.

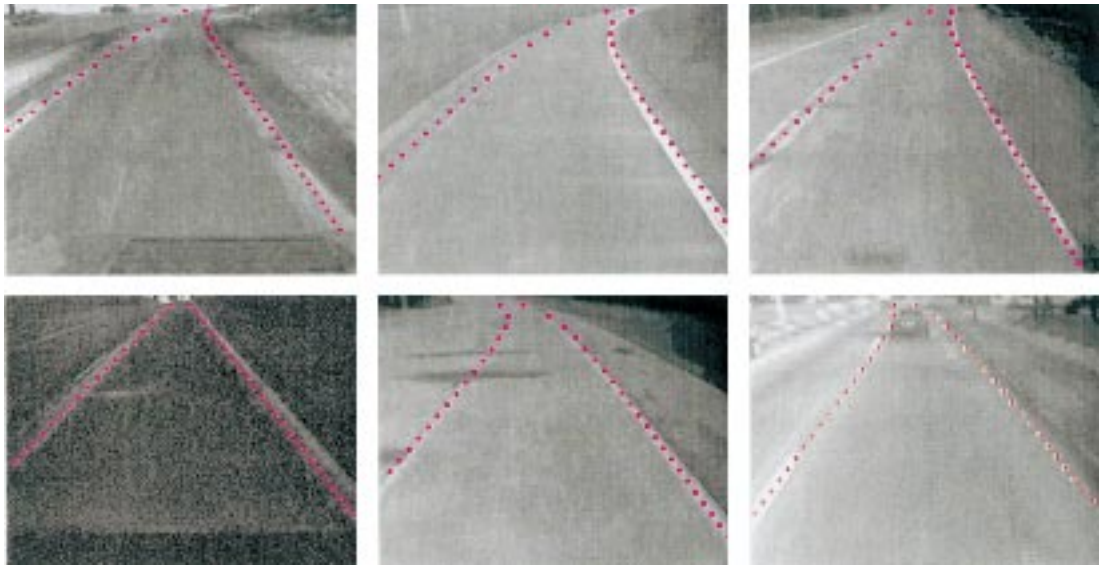

Fig. 9. Examples of LOIS detecting the lanes correctly.

for a more detailed description), the results of which are shown in Fig. 9.

Despite LOIS' robustness, it still has a problem common with most edge-based lane detection systems. LOIS has a tendency to be 'distracted' or 'pulled' away from the true lane markers by the presence of strong and structured edges such as those created by a vehicle outline, as discussed in Section 1.4 and illustrated in Fig. 8. The resulting unreliability of the curvature estimate could be an issue if LOIS is to be integrated into a LDW system, where accurate knowledge of the lane position far from the vehicle (~100 m.) is important. This could also be an issue if LOIS was used to determine the lane relevancy of an obstacle detected in front of the vehicle for an ICC or CW system.

3. CLARK

The CLARK algorithm detects obstacles and lanes by fusing information from the radar sensor as well as the visual sensor. CLARK has two distinct steps:

- first, CLARK uses a deformable obstacle template to determine the position and extent of the vehicle/obstacle ahead;
- next, CLARK incorporates the information gathered in step 1 into the LOIS lane detection algorithm by using a combined obstacle/lane likelihood function.

This section provides a detailed description of these two steps of CLARK.

A note regarding the data used in this paper is in order. A significant portion of the data used in this paper was gathered at the National Highway Traffic Safety Administration's (NHTSA's) test track facility at the Transportation Research Center (TRC), East Liberty, OH. Using DASCAR,[5] data was simultaneously collected from two forward-looking sensors, namely, a radar and a visual sensor [46,47].

3.1. Obstacle detection using a radar sensor

As mentioned earlier, the proximity/range information regarding the vehicle/obstacle ahead that is used in this paper comes from a radar sensor. Shown in Fig. 10 are several examples of the radar sensor's output. Notice that the sensor performance is good when the vehicle/obstacle is directly ahead. However, when the vehicle/obstacle is not directly ahead—because the road ahead curving to the left or the right, for example—the radar sensor's performance is no longer good. As previously discussed, there are a number of 'trouble scenarios' for radar-based ICC/CW systems, including the one depicted in Fig. 10, that lead to instances of false alarms, i.e. the radar sensor reports that the lead vehicle is much close or further away than it actually is.

There are several methods to eliminate such false alarms. Shown in Fig. 11 is an example of using a standard Kalman filter for post-processing the radar sensor's output. Notice how the radar sensor has a tendency to sometimes 'totally miss' the vehicle ahead, and how that situation is somewhat rectified by the use of a post-filter. Unfortunately, filtering is not sufficient, especially if the vehicle ahead is being persistently missed by the radar sensor (see Fig. 12). A more reliable solution to this problem involves either the use of a scanning radar [9] or a multiple beam radar [19]. In this paper, we contend that rather than resort to such expensive

[5] A vehicle-mounted portable system developed by the NHTSA and the Oak Ridge National Laboratory for acquiring information regarding driver performance and behavior.

Fig. 10. Examples of determining the range/proximity of a vehicle ahead using radar in situations where the radar performance is good (left two) and not good (right two).

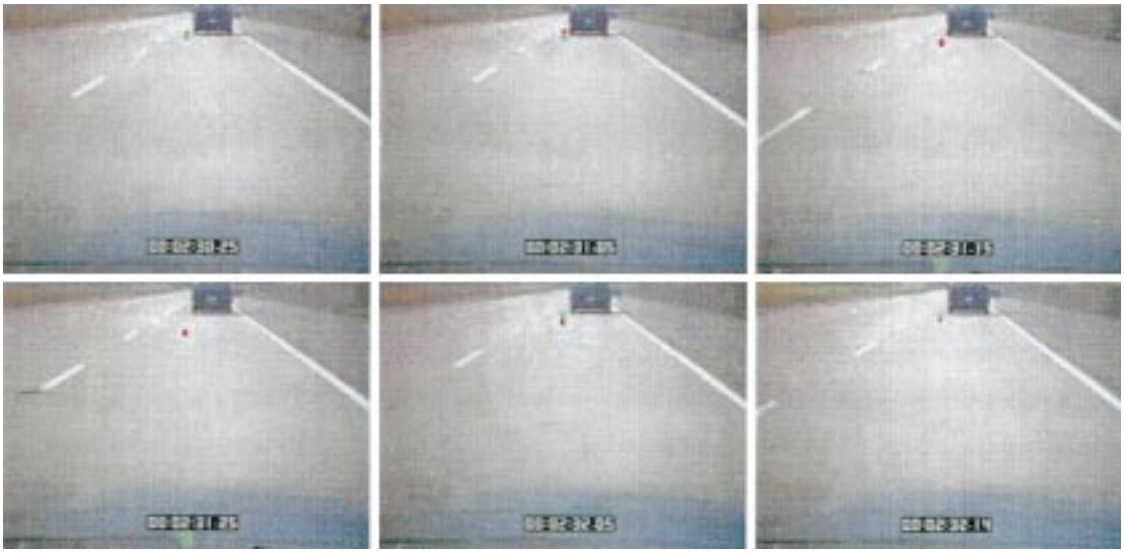

Fig. 11. Reducing impulsive errors in the radar sensor's output (green dot) using a Kalman filter (red dot).

modifications of the narrow beam radar, an alternative (and considerably cheaper) method for robust obstacle detection involves the mere addition of a low-cost visual sensor. This visual sensor has the advantage of also providing lane information (and hence lane relevancy of obstacles), something that neither scanning nor multiple-beam radars provide.

3.2. Incorporating visual information into obstacle detection

CLARK uses the information contained in the visual image's intensity gradient[6] and color fields in order to reliably detect obstacles. A rectangular obstacle template is formed. This template is deformed by varying its left, right, and bottom edges and then matched to the visual image's intensity gradient field. Deformations that keep the obstacle template close to where the radar sensor's output are deemed more probable (using a novel data-derived prior probability density) than those that move the template farther away. The various elements of this obstacle detection scheme are discussed in more detail in a sequel.

CLARK begins by Kalman filtering the radar sensor's output. This step is necessary to eliminate impulsive errors in the sensor output and is based on the following two (state and observation) equations:

$$r(t+1) = [1\ \Delta t]\begin{bmatrix} r(t) \\ \dot{r}(t) \end{bmatrix} + w(t) \tag{11}$$

$$d(t) = r(t) + v(t)$$

where $r(t)$ is the true (unknown) range of the vehicle/obstacle ahead, $\dot{r}(t)$ is the vehicle's/obstacle's true (unknown) range rate, $d(t)$ is the observed range of the vehicle/obstacle ahead, Δt is the time interval between observations, and both $w(t)$ are $v(t)$ are two empirically determined iid Gaussian random processes. Given the $d(t)$ (observations), the Kalman filter causually estimates the $r(t)$'s and $\dot{r}(t)$'s (the states).

CLARK treats $\hat{r}(t)$ (the Kalman estimate of $r(t)$) as the quantity that denotes the range/proximity of the vehicle/obstacle ahead in the image frame indexed by t, and uses the difference between $\hat{r}(t)$ and $d(t)$ in order to bias the deformations of the rectangular obstacle template in that frame. Vehicles/obstacles detected by the radar are always biased to lie exactly in the middle of the radar beam, but are

[6] Note that LOIS uses the intensity gradient field as well, and so this information is already available.

Fig. 12. A situation where Kalman filtering (red dot) of the radar sensor's output is ineffective.

allowed to vary their lateral position over one lane width subject to a penalty.

More specifically, let (T_b,T_l,T_w) denote the three deformable parameters of the rectangular obstacle template corresponding to the position of its bottom and left edges and the extent of its width in the image plane, $[x_r(t),x_c(t)]$ the corresponding center of the deformed template image plane, and $[y_r(t),y_c(t)]$ the position of the obstacle in the image plane as detected by the radar sensor and subsequently Kalman filtered. CLARK assumes that:

$$P(T_b, T_l, T_w|[y_r(t), y_c(t)]) \propto \exp\left\{-\left[\frac{(x_r(t)-y_r(t))^2}{\sigma_r^2(t)} + \frac{(x_c(t)-y_c(t))^2}{\sigma_c^2}\right]\right\} \times \frac{\tan^{-1}[5*(T_w-T_{min})]-\tan^{-1}[5*(T_w-T_{max})]}{\tan^{-1}[2.5*(T_w-T_{min})]-\tan^{-1}[2.5*(T_w-T_{max})]} \quad (12)$$

where $\sigma_r^2(t)$ is a running estimate of $\hat{x}(t) - d(t)$'s variance, and σ_c^2 is equal to the image plane value of one lane width (3.2 m), taking into account the foreshortening effects of the ground-plane to image-plane transformation. The ratio of $\tan^{-1}$ in the above equation constrains the obstacle template's width to be no less than T_{min} (one half of a lane) and no more than T_{max} (one full lane) in the image plane.

Next, using the intensity gradient field of the observed visual image, for each hypothesis of (T_b,T_l,T_w) CLARK determines the degree to which that particular position/deformation of the obstacle template matches the image. This determination is made via a matching function that prefers deformations that place the template over portions of the visual image that have a strong intensity gradient field and whose orientation is perpendicular to the template edges:

$$P(\text{Observed Image}|T_b, T_l, T_w) \propto \sum_{i,j\in\text{bottom edge}} \text{GradMag}_{i,j} * |\sin(\text{Gradortn}_{i,j})| + \sum_{i,j\in\text{left and right edges}} \text{GradMag}_{i,j} * |\cos(\text{GradOrtn}_{i,j}| \quad (13)$$

The sum over the left and right edges in the above equation is not actually performed over the entire left/right edges, but only over a hand full of pixels close to the bottom.

The probabilities $P(T_b, T_l, T_w|[y_r(t), y_c(t)])$ and $P(\text{Observed image}|T_b, T_l, T_w)$ from Eqs. (12) and (13) are combined using Bayes' rule, and the obstacle detection problem is reposed as:

$$\begin{aligned}&\underset{T_b,T_l,T_w}{\text{argmax}}\, P(T_b, T_l, T_w|[y_r(t), y_c(t)], \text{Observed Image})\\ &= \underset{T_b,T_l,T_w}{\text{argmax}}\, P(\text{Observed Image}|T_b, T_l, T_w)\\ &\quad \times P(T_b, T_l, T_w|[y_r(t), y_c(t)])\end{aligned} \quad (14)$$

This yields positive results,[7] and considerably improves the position of the obstacle as seen by the radar sensor (see Fig. 13). While this is encouraging, instances when the method failed were found to be troublesome—for example, the method has trouble detecting the obstacle correctly when the image contains strong extraneous edges or when the obstacle occupies only a small area on the image plane (see Fig. 14).

To overcome such failures associated with detecting obstacles using the intensity gradient field alone, the visual image's color field is used. For each hypothesis/deformation of the obstacle template, obtained by varying T_b,T_l,T_w, let S_1 and S_2 denote the collection of pixels inside and outside (a four pixel-wide band) of the template—the elements of S_1 and S_2 are three-dimensional (corresponding to the red, blue and green channels of the observed image). Let M_1, M_2 and Σ_1, Σ_2 denote the mean and covariance (estimated by sample averages) of S_1 and S_2, respectively. Let $\mathbf{w}$ denote the linear projection of pixels in S_1 and S_2 onto a single dimension, and let m_1, m_2 and σ_1, σ_2 denote the corresponding projections of M_1, M_2 and Σ_1, Σ_2, respectively. When the projection operator $\mathbf{w}$ exactly equals $(\Sigma_1 + \Sigma_2)^{-1}(M_1 - M_2)$, the projection-plane variance-normalized distance $[m_1 - m_2]^2/(\sigma_1^2 + \sigma_2^2)$ is maximized. Such a $\mathbf{w}$ is called the Fisher discriminant [48,49] and the corresponding variance-normalized distance is called the Fisher distance between S_1 and S_2. This Fisher distance is used to enhance

[7] This method was tested on more than 1600 images and found to detect the vehicle ahead more than 90% of the time.

Fig. 13. Obstacle detection using gradient information alone. Left: observed visual image-radar output in green. Middle: the intensity gradient field. Right: the obstacle detected by CLARK—red box.

the matching function in Eq. (13):

$$P(\text{Observed Image}|T_b, T_l, T_w) = \text{FishDist}(T_b, T_l, T_w) \times \left\{ \sum_{i,j,\in\text{bottom edge}} \text{GradMag}_{i,j} * |\sin(\text{GradOrtn}_{i,j})| + \sum_{i,j\in\text{left and right edges}} \text{GradMag}_{i,j} * |\cos(\text{GradOrtn}_{i,j})| \right\} \quad (15)$$

The obstacle is detected again by performing the maximization in Eq. (14), with this new function.[8] The results are much improved (see Figs. 15 and 16).

3.3. The combined likelihood

Once the obstacle has been detected, knowledge of its location can be integrated into the LOIS lane detection algorithm. The objectives for doing this are two-fold:

1. registration of obstacle's position in order to determine its lane relevancy;
2. increasing LOIS' accuracy.

The first objective is simple—LOIS estimates the offset, orientation, and curvature of both the left and right lanes. Using these, the exact position of both the left and right lanes can be determined at any chosen distance from the image plane. Therefore, given the range and extent of an obstacle, its lane relevancy is easily determined, provided LOIS' output is accurate. Objective 2, increasing LOIS' accuracy using the obstacle detection results, is also simple. By a straightforward masking technique (see Section 1), LOIS' accuracy can be considerably improved, provided the obstacle detection results are accurate. Unfortunately, the qualification 'simple' assumes that both the lane's shape and the obstacle's position and extent are accurately determined. If either of the estimations have any error, then such a subsequent 'simple' integration of their result will give rise to unreliable results (see Fig. 17).[9]

A better strategy, and the one adopted in this paper, is to use both the lane and obstacle information together via a combined likelihood probability. This new likelihood probability is a product of the RHSs of Eqs. (9) and (15), and it determines the degree to which deformations of both the lane and obstacle templates together match the features of the observed image:

$$\begin{aligned} &P(\text{Observed Image}|k', b'_{\text{LEFT}}, b'_{\text{RIGHT}}, vp, T_b, T_l, T_w) \\ &= \left\{ \sum_{i,j} \text{GradMag}_{i,j} f(\alpha_1, \text{Dist}_{i,j}) * f(\alpha_2, \cos[\text{GradOrtn}_{i,j} - \text{TempTgt}]) \right\} \times \text{FishDist}(T_b, T_l, T_w) \\ &\times \left\{ \sum_{i,j\in\text{bottom edge}} \text{GradMag}_{i,j} * |\sin(\text{GradOrtn}_{i,j})| + \sum_{i,j\in\text{left and right edges}} \text{GradMag}_{i,j} * |\cos(\text{GradOrtn}_{i,j})| \right\} \end{aligned} \quad (16)$$

This new likelihood is combined with a new prior (a product of the prior probabilities in Eqs. (8) and (12))

$$\begin{aligned} &P(k', b'_{\text{LEFT}}, b'_{\text{RIGHT}}, vp, T_b, T_l, T_w|[y_r(t), y_c(t)]) \\ &\propto (a\tan[b'_{\text{RIGHT}} - b'_{\text{LEFT}} - 1] - a\tan[b'_{\text{RIGHT}} - b'_{\text{LEFT}} - 3]) \times \exp\left\{ -\left[\frac{(x_r(t) - y_r(t))^2}{\sigma_r^2(t)} + \frac{(x_c(t) - y_c(t))^2}{\sigma_c^2} \right] \right\} \\ &\times \frac{\tan^{-1}[5 * (T_w - T_{\min})] - \tan^{-1}[5 * (T_w - T_{\max})]}{\tan^{-1}[2.5 * (T_w - T_{\min}] - \tan^{-1}[2.5 * (T_w - T_{\max})]} \end{aligned} \quad (17)$$

Obstacles and lanes are detected by finding a local maximum of the new seven-dimensional posterior pdf $P(k', b'_{\text{LEFT}}, b'_{\text{RIGHT}}, vp, T_b, T_l, T_w|[y_r(t), y_c(t)]$, Observed Image). Note:

- So that the same pixel does not contribute to both terms of the likelihood probability simultaneously (i.e. so that a pixel in the observed image is not simultaneously both a lane and an obstacle), any pixel that is contributing to the

[8] The Fisher distance is scaled to account for the range-dependent variation in the actual distance between pixels.

[9] The plots in Fig. 17 were generated by calculating the RMS error between the detected lanes and the hand-picked ground truth for various look ahead distances from the host vehicle. The database used contained 41 images.

Fig. 14. Problem situations when obstacles are detected by CLARK, using only the gradient field information. Left: Strong extraneous edges; and right: vehicle ahead having an internal edge structure.

Fig. 15. Obstacle detection using intensity gradient field—left, and adding Fisher distance—right.

summation in one of the terms does not contribute to the other.

- So that this mutual exclusion does not cause a bias towards unduly long lanes, CLARK normalizes the new likelihood probability in Eq. (8), by a factor that equals the ratio of the # of pixels along a certain lane template hypothesis to the number of pixels along that lane that are not part of the obstacle template hypothesis.

The lane detection results using CLARK are contrasted to the alternatives (standard LOIS and LOIS' likelihood contributions modified by a separately detected obstacle) in Fig. 17 in order to emphasize the improvement in accuracy.[10] In Fig. 18, some sample results of both lane and obstacle detection results using CLARK are presented.

[10] For an image of size 160×120, LOIS takes about fifteen minutes to exhaustively search over the space of all lane shape parameters, the addition of the obstacle parameters to the search space makes CLARK significantly slower—it takes approximately 2 h. All the computations were performed on a desktop PC with a 133 MHz CPU and 80 Mbytes of RAM.

4. Concluding remarks

This paper described CLARK, a method for detecting vehicles and lanes through the fusion of radar and visual information. CLARK has three components:

1. A vehicle detection component—Range information was used to localize the search for the target in the visual image. The vehicle detection problem was re-posed as a three-parameter local Bayesian optimization problem that used the visual image intensity gradient field along with a color-based linear discriminant and a deformable rectangular shape model for vehicles.
2. Lane detection was the second component—Using a slightly modified version of the Likelihood Of Image Shape (LOIS) algorithm, lanes were detected separately without incorporating any vehicle detection results. The LOIS algorithm uses a likelihood that encodes the knowledge that lane edges should be in portions of the image where the intensity gradient is large in magnitude and whose orientation is perpendicular to the lane edge.
3. The final component was the combined likelihood—The detected vehicle from the first component is used to

Fig. 16. Examples of obstacle detection using both the intensity gradient and the color fields.

refine the lane shape estimation of the second component, and in the process the position of the detected vehicle is allowed to vary as well. The simultaneously best estimate of both the vehicle and lane positions was found through a combined likelihood function. The area corresponding to the vehicle's hypothesized location in the gradient field was masked so that gradient pixels counted in the vehicle's portion of the likelihood were not counted in LOIS' portion, and vice versa. This combined vehicle and lane likelihood function was locally maximized by allowing the vehicle and lane parameters to vary within a narrow range around their separately determined values.

Several experimental results illustrating the efficacy of each of these three components were presented in this paper. Some possible future work includes:

- An extension of CLARK to detect multiple targets. As technology advances, radar and laser radar units will become more sophisticated and cheaper. It is reasonable

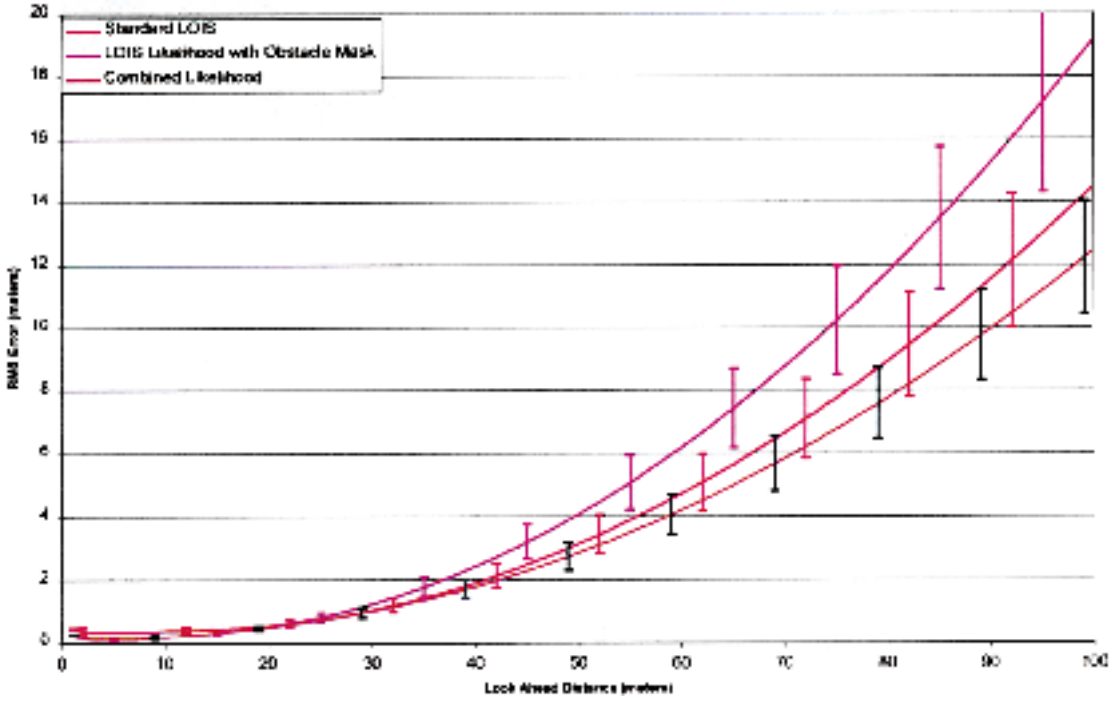

Fig. 17. A comparison of lane detection results using the standard LOIS, LOIS with a separately detected obstacle masking the gradient field, and CLARK.

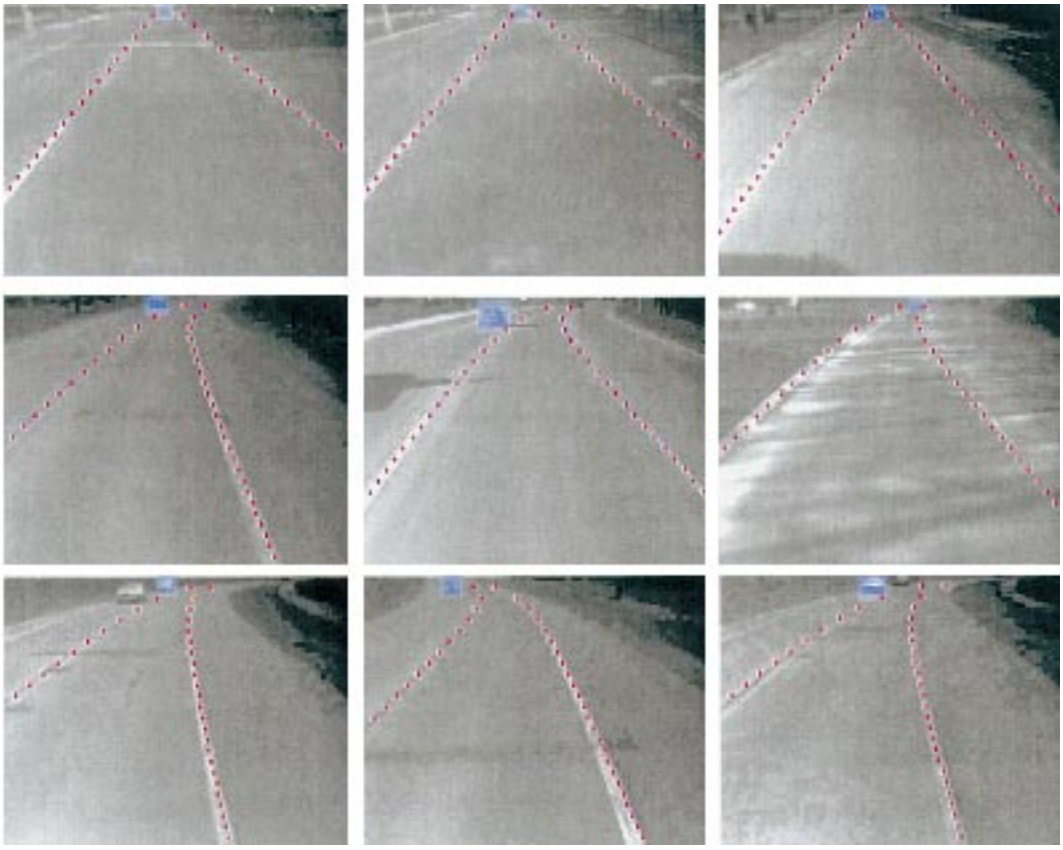

Fig. 18. A sample of lanes and obstacles detected using CLARK.

to assume that affordable systems will be designed to detect multiple obstacles, and it will be necessary to fuse all of these detections with the visual image in order to determine their lane relevancy.

- A further exploration of the manner in which the gradient and color information is combined. Rather than use the Fisher (maximum) discriminant, perhaps an alternative such as the minimum discriminant could be used to yield a max–min obstacle detection scheme, much in the spirit of many traditional robust detection theories—see [50].
- A complete optimization of CLARK's algorithm to increase its speed of computation.

References

[1] American Automobile Manufacturers Association (AAMA), Motor Vehicle Facts & Figures 1996, Government Affairs Division of the American Automobile Manufacturers Association, Detroit, MI, 1996.
[2] L.J. Blincoe, The economic cost of motor vehicle crashes, NHTSA Plans and Policy Technical Report, US Department of Transportation, Washington, 1994.
[3] X. Chu, The effects of age on the driving habits of the elderly, Evidence from the 1990 National Personal Transportation Study, DOT-T-95-12, Office of University Research and Education Research and Special Programs Administration, Washington, DC, October 1994.
[4] F.S. Washington, Consumers downgrade airbags as a reason to buy, Automotive News, 10 February, 1997, p. 56.
[5] National Highway Safety Administration, Report to Congress on the National Highway Safety Administration ITS Program, Program Progress During 1992–1996 and Strategic Plan for 1997–2002, January 1997.
[6] D.J. LeBlanc, G.E. Johnson, P.J.Th. Venhovens, G. Gerber, R. DeSonia, R.D. Ervin, C. Lin, A.G. Ulsoy, T.E. Pilutti, CAPC: a road-departure prevention system, IEEE Control Systems Magazine 16 (6) (1996) 61–71.
[7] M. Chen, T. Jochem, D. Pomerleau, AURORA: a vision-based roadway departure warning system, Proceedings of the IEEE Conference on Intelligent Robots and Systems (1995).
[8] S. Lakshmanan, K. Kluge, LOIS: a real-time lane detection algorithm, Proceedings of the 30th Annual Conference on Information Sciences and Systems (1996).
[9] L.H. Eriksson, Ås. Bengt-Olof, A high performance automotive radar for automatic AICC, IEEE Aerospace and Electronic Systems Magazine 10 (12) (1995) 13–18.
[10] P. Ganci, S. Potts, F. Okurowski, A forward looking automotive radar sensor, Proceedings of the Intelligent Vehicles Symposium (1995) 321–325.
[11] A. Suzuki, N. Yasui, N. Nakano, M. Kaneko, Lane recognition system for guiding of autonomous vehicle, Proceedings of the Intelligent Vehicles Symposium (1992) 196–201.
[12] J. Woll, Vorad collision warning radar, Proceedings of the IEEE International Radar Conference (1995) 369–372.
[13] S.K. Kenue, LANELOK: detection of lane boundaries and vehicle tracking using image-processing techniques—Parts I and II, Proceedings, SPIE Mobile Robots IV (1989) 221–244.
[14] K.C. Kluge, Extracting road curvature and orientation from image edge points without perceptual grouping into features, Proceedings of the Intelligent Vehicles Symposium (1994) 109–114.

[15] A. Polk, R. Jain, A parallel architecture for curvature-based road scene classification, Roundtable Discussion on Vision-Based Vehicle Guidance (in conjunction with IROS), July 1990.
[16] D. Pomerleau, T. Jochem, Rapidly adapting machine vision for automated vehicle steering, IEEE Expert 11 (2) (1996) 19–27.
[17] S. Tokoro, Automotive application systems of a millimeter-wave radar, Proceedings of the IEEE Intelligent Vehicles Symposium (1996) 260–265.
[18] S. Azevedo, T. McEwan, Microwave impulse radar, IEEE Potentials 16 (2) (1997) 15–20.
[19] D. Langer, T. Jochem, Fusing radar and vision for detecting, classifying and avoiding roadway obstacles, Proceedings of the IEEE Intelligent Vehicles Symposium (1996) 333–338.
[20] J. Borenstein, Y. Koren, Real-time obstacle avoidance for fast mobile robots, IEEE Transactions on Systems, Man, and Cybernetics 19 (5) (1989) 1179–1187.
[21] D. Langer, C. Thorpe, Range sensor based outdoor vehicle navigation, collision avoidance, and parallel parking, Autonomous Robots 2 (1995) 147–161.
[22] E.D. Dickmanns, B. Mysliwetz, T. Christians, An integrated spatio-temporal approach to automatic visual guidance of autonomous vehicles, IEEE Transactions on Systems, Man and Cybernetics 20 (6) (1990) 1273–1284.
[23] A. Kuhnle, Symmetry-based recognition of vehicle rears, Pattern Recognition Letters 12 (4) (1991) 249–258.
[24] U. Regensburger, V. Graefe, Obstacle classification for obstacle avoidance, Proceedings of SPIE—Mobile Robots V 1388 (1990) 112–119.
[25] U. Regensburger, V. Graefe, Visual recognition of obstacles on roads, IEEE/RSJ/GI International Conference on Intelligent Robots and Systems (1994) 980–987.
[26] B. Heisele, W. Ritter, Obstacle detection based on color blob flow, Proceedings of the IEEE Intelligent Vehicles Symposium (1995) 282–286.
[27] S. Buluswar, Color machine vision for autonomous vehicles, Department Of Computer and Information Sciences Technical Report, University of Massachusetts–Amherst, 1997.
[28] M. Bertozzi, A. Broggi, Real-time lane and obstacle detection on the GOLD system, Proceedings of the IEEE Intelligent Vehicles Symposium (1996) 213–218.
[29] K. Saneyoshi, 3-D image recognition system by means of stereoscopy combined with ordinary image processing, Proceedings of the IEEE Intelligent Vehicles Symposium (1994) 13–18.
[30] L. Raffaelli, E. Stewart, Millimeter automotive radars: the markets, technologies, and production costs, Proceedings of the SPIE—Intelligent Vehicle Highway Systems 2344 (1994) 129–133.
[31] A.G. Stove, Linear FMCW radar techniques, IEE Proceedings, Part F: Radar and Signal Processing 139 (5) (1992) 343–350.
[32] H. Araki, K. Yamada, Y. Hiroshima, T. Ito, Development of rear-end collision avoidance system, Proceedings of the IEEE Intelligent Vehicles Symposium (1996) 224–229.
[33] C. Thorpe, O. Amidi, J. Gowdy, M. Hebert, D. Pomerleau, Integrating position measurement and image understanding for autonomous vehicle navigation, Robotics Institute Technical Report, Carnegie Mellon University, 1991.
[34] M. Beauvais, C. Kreucher, S. Lakshmanan, Building world models for mobile platforms using heterogeneous sensor fusion and temporal analysis, Proceedings of the First IEEE Intelligent Transportation Systems Conference (1997).
[35] K. Jörg, World modeling for an autonomous mobile robot using heterogeneous sensor information, Robotics and Autonomous Systems 14 (1995) 159–170.
[36] Y. Wu, J. Yang, K. Liu, Obstacle detection and environment modeling based on multisensor fusion for robot navigation, Artificial Intelligence in Engineering 10 (1996) 323–333.
[37] B. Heisele, H. Neef, W. Ritter, R. Schneider, G. Wanielik, Object detection in traffic scenes by a color video and radar data fusion approach, Proceedings of the First IEEE Australian Data Fusion Symposium (1996) 48–52.
[38] D. Grimmer, Finding straight edges in radar images using deformable templates, Master's Thesis, Department Of Electrical and Computer Engineering, University of Michigan–Dearborn, 1993.
[39] K. Kaliyaperumal, LEXLUTHER: an algorithm for road edge detection in radar images, Master's Thesis, Department Of Electrical and Computer Engineering, University Michigan–Dearborn, 1997.
[40] K. Hashimoto, S. Nakayama, T. Saito, N. Oono, S. Ishida, K. Unoura, J. Ishii, Y. Okada, An image-processing architecture and a motion control method for an autonomous vehicle, Proceedings of the Intelligent Vehicles Symposium (1992) 213–218.
[41] K.C. Kluge, Performance evaluation of vision-based lane sensing: some preliminary tools, metrics and results, IEEE Conference on Intelligent Transportation Systems (1997).
[42] C. Kreucher, S. Lakshmanan, LANA: a lane extraction algorithm that uses frequency domain features, IEEE Transactions on Robotics and Automation (1999).
[43] P.N. Strenski, S. Kirkpatrick, Analysis of finite length annealing schedules, Algorithmica 6 (1991) 346–366.
[44] K. Kluge, S. Lakshmanan, A deformable template approach to lane detection, Proceedings of the Intelligent Vehicles '95 Symposium (1995) 54–59.
[45] K. Kluge, S. Lakshmanan, Lane boundary detection using deformable templates: effects of image subsampling on detected lane edges, in: S.Z. Li, D.P. Mital, E.K. Teoh, H. Wang (Eds.), Recent Developments in Computer Vision, 1996.
[46] R. Carter, F. Barickman, M. Goodman, DASCAR sensor suite and video data system, Proceedings of the SPIE—Transportation Sensors and Controls: Collisions Avoidance, Traffic Management, and ITS 2902 (1996) 250–259.
[47] R. Carter, P. Spelt, F. Barickman, Feasibility of a portable data acquisition system for driver performance testing, Proceedings of the Human Factors and Ergonomics Society 40th Annual Meeting 2 (1996) 1017–1021.
[48] R. Duda, P. Hart, Pattern Classification and Scene Analysis, Wiley, New York, 1973.
[49] H. Stark, J.W. Woods, Probability and Random Processes, Prentice-Hall, Englewood Cliffs, NJ, 1994.
[50] S.A. Kassam, H.V. Poor, Robust techniques for signal processing: a survey, Proceedings of the IEEE 73 (3) (1985) 433–481.